

In silico and *in vitro* evaluation of compounds from Methanol whole extracts of *Solanum aculeastrum* Dunal berries against benign prostatic hyperplasia and prostate cancer

Gift Crucifix Pender^{1,2,*}, Bernard Guyah¹, Peter G Mwitari³, Mercy Jepkorir³, Inyani John L. Lagu⁴ and James Ombaka⁵

¹ Department of Biomedical Sciences and Technology, School of Public Health and Community Development, Maseno University, Kenya.

² Department of Pharmacology and Toxicology, School of Medicine and Pharmacy, College of Medicine and Health Sciences, University of Rwanda, Kigali, Rwanda.

³ Center for Traditional Medicine and Drug Research, Kenya Medical Research Institute (KEMRI), Nairobi, Kenya.

⁴ Pan African University for Basic Sciences, Technology, and Innovation (PAUSTI), Nairobi, Kenya.

⁵ Department of Pharmaceutical Sciences, School of Public Health and Community Development, Maseno University, Kenya.

International Journal of Science and Research Archive, 2024, 13(01), 193–217

Publication history: Received on 20 July 2024; revised on 01 September 2024; accepted on 03 September 2024

Article DOI: <https://doi.org/10.30574/ijrsra.2024.13.1.1616>

Abstract

Background: This study evaluated anti-prostate potentials of compounds from methanol extract of *Solanum aculeastrum* Dunal berries (MESADB) against benign prostatic hyperplasia (BPH) and prostate cancer (PC).

Methods: We used Swiss ADME and pKCSM tools to select drug-like candidates from MESADB. DisGeNET and related databases were used to identify targets for compounds of MESADB, BPH and PC. Molecular roles, biological processes, cellular components involved, and crucial pathways associated with biological processes of gene enrichment were obtained using Gene Ontology (GO) & Kyoto Encyclopedia of Genes and Genomes (KEGG), respectively. Docking was achieved using VINA tool. Antiproliferative and gene expression profiling were determined using 3-[4,5-dimethylthiazol-2-yl]-2,5-diphenyltetrazolium bromide (MTT) bioassay, and RT-qPCR respectively, and data analyzed using Graph Pad Prism (version 8.4).

Results: Three ideal drug-like candidates [Undecane; D-Arabinitol; and 9-Oxabicyclo [3.3.1] nonan-2-one,6-hydroxy-] were identified. Key targets included TLR4, PTGS2, STAT3, ESR1, MTOR, SRC, MMP9, HDAC1, AKT1 and EGFR. GO analysis revealed key targets were mainly enriched in 601 biological processes (BP), 53 molecular function (MF) and 24 cellular components (CC) terms ($p < 0.05$). KEGG analysis presented pathways for cancer, pathway of proteoglycans in cancer, amongst others. Docking revealed [D-Arabinitol; and 9-Oxabicyclo [3.3.1] nonan-2-one,6-hydroxy-] demonstrated high binding affinity with PTGS2 and EGFR. MESADB significantly ($p < 0.0001$) inhibited growth of DU-145 cells with IC_{50} value and selectivity index of 5.11 $\mu\text{g/ml}$ and 14.84, respectively, while sparing Vero CCL-81 cells. There were significant ($p < 0.0001$) downregulations of EGFR, PTGS2 and BCL-2, in treated DU-145 cells compared to control.

Conclusion: MESADB possesses antiprostatae potentials.

Keywords: *In silico*; *In vitro*; Methanol-extract-of-*Solanum-aculeastrum*-Dunal-berries; Benign prostatic hyperplasia; Prostate cancer

* Corresponding author: Gift Crucifix Pender; Email: crucifixpender@gmail.com

1 Introduction

Phytotherapy has continued to thrive over the years as a panacea to various diseases that have posed challenges to humanity due to their perceived cost-effective and relatively safer profiles [1, 2]. Phytochemicals present in extracts of medicinal plants have demonstrated potentials against different ailments and have been employed in traditional management of disease conditions [3]. Benign prostatic hyperplasia (BPH) is an age-related condition which affects approximately 70% of men who have attained 70 years and above [4], and it is characterized by abnormal enlargement of the prostate which results to manifestations of lower urinary tract syndromes (LUTs) [5]. The complications of BPH could lead to urinary discomforts which includes urgent and frequent passing of urine, nocturia, hesitancy and incomplete bladder emptying all of which affects quality of life of the affected patients [6–8]. The prevalence of BPH ranges from 8% in 31–40 years old men, to more than 80% in men older than age 80 [9]. Even though BPH is an abnormal enlargement of the prostate gland caused by cellular hyperplasia, which is non-malignant, it could cause complications and even progress to prostate cancer which could manifest as high-grade PC [10–12]. BPH was found to be associated with 2.9-fold increased risk of occurrence of prostate cancer [13].

Prostate cancer which is a life-threatening malignant disease of the prostate gland, also age related, was ranked the second most common cancer that affects the elderly men and also the fifth cause of cancer-associated deaths globally [14]. World over, about 1,414,259 new cases were reported in 2020, with 77,300 reported new cases in Africa [15], which due to the increase in the aging population, has been estimated to increase to almost 2.3 million new cases and 740,000 deaths by 2040 [16]. Various explanations regarding the pathogenesis of these conditions that affect the prostate gland have been provided by researchers. Hormones, inflammation, and metabolic syndrome have all been implicated in both BPH and PC [10, 17–20]. The involvement of the enzyme, 5 α -reductase which converts the androgen, testosterone to its active form, dihydrotestosterone (DHT), believed to cause stimulation of the prostate gland leading to abnormal enlargement [21] constitutes a vital aspect of the pathogenesis of these hormonal imbalance conditions. Improper regulation of apoptotic activity within the cell cycle could lead to abnormal surge in the number of cells, eventually progressing to uncontrolled growth of the prostate gland [22]. It is well known that inflammation is a risk factor for both BPH and prostate cancer [23, 24]. Chronic inflammation has also been implicated in the pathogenesis of BPH as inflammatory cytokines and chemokines released during inflammatory process that may ensue as a result of infection could result in the abnormal growth of the prostatic epithelial and stromal cells [25, 26].

Apart from the fact that the conventional drugs indicated for management of these conditions such as 5 α -reductase inhibitors and α -blockers, have to be used for a longer duration without proffering a significant curative solution [4], they are associated with disturbing side effects, such as vascular deficits, sexual dysfunction, hyperglycemia, and erectile dysfunction [27, 28]. Hence, more attention is being directed to the use of herbal products which appear more promising, have little or no adverse effects, more tolerable and are less expensive [29–31].

Solanum aculeastrum Dunal, belonging to the family, Solanaceae, is a plant native to tropical Africa and South Africa which grows in a variety of terrains and climatic conditions [32, 33]. Preparations from the leaves and berries are folklorically employed in the management of disease conditions including cancer, stomach disorders, gonorrhoea and indigestions [32, 34]. The steroidal alkaloid solamargine, from the berries of *S. aculeastrum* Dunal crude extract and aqueous fraction was reported to have demonstrated potent non-selective cytotoxic and inhibitory activities against different cancer types [35]. Also, the fruits, root barks and leaves have been used against cervical and skin cancers [36]. The cytotoxic activities of saponins and carpesterol from berries of *S. aculeastrum* Dunal were also documented recently against three human cancer cell lines including breast cancer (MCF-7), lung cancer (NCI-H460), and cervical cancer (Hela) [37].

In a prior study, we carried out an exhaustive and comprehensive phytochemical screening and GC-MS profiling of methanol whole extract and solvent fractions of the berries of *S. aculeastrum* Dunal, in which 32 bioactive compounds were identified from the methanol extract [38]. In the present study, we aimed to further evaluate the bioactive compounds identified by GC-MS analysis from the methanol whole extracts through *in silico* prediction of the targets involved in their activities involving molecular docking, with a focus to explore their potentials against prostate cancer (PC) and benign prostatic hyperplasia (BPH), prediction of the physicochemical properties, pharmacokinetic and toxicological profiles as well as *in vitro* laboratory evaluation to validate the anti-prostate potentials.

2 Materials and Methods

2.1 *In silico* studies

2.1.1 Prediction of physicochemical properties of drug candidates using Swiss ADME Tool

Following successful access to PubChem (<https://pubchem.ncbi.nlm.nih.gov/>), the bioactive compounds in the MESADB identified by the Canonical Simplified Molecular Input Line Entry System (SMILES) of the GC-MS were retrieved. Succeeding the retrieval was the submission of the SMILES to the Swiss ADME tool (<http://www.swissadme.ch/index.php>) for prediction of the drug-likeness and bioactive compounds' physicochemical properties. Parameters such as the total polar surface area, blood-brain barrier, drug metabolizing enzymes such as cytochrome P450s (CYP2D6 and CYP3A4) served as the basis for prediction coupled with the application of the Lipinski's rule of five (RO5) which states that a drug candidate should have a number of rotatable bonds of < 10; a number of hydrogen bond donors of < 5; a number of hydrogen bond acceptors of < 10; a lipophilicity (Log P) value of < 5 and should have a molecular weight of < 500g/mol. The principle is that a molecule or drug candidate that fails to meet two or more of the 5 components is predicted to be a non-orally accessible drug [39]. The knowledge that the polar atom of a molecule contributes to the topological polar surface area (TPSA), could aid in the prediction of the transport and distribution of the drug [40]. Molecules or drugs that possess abilities to cross the blood brain barrier (BBB) may be harmful to the nervous system. Moreso, a drug candidate is not expected to inhibit drug metabolizing hepatic enzymes which are majorly the cytochrome P450 enzymes especially CYP2D6 and CYP3A4 that are extensively involved in the metabolism of a wide variety of drugs [40]. Thereafter, we used the pKCSM tool to predict the pharmacokinetic properties and toxicity tendencies (ADMET) of our drug compounds (<https://biosig.lab.uq.edu.au/pkcsm/prediction>).

2.1.2 Candidate targets identification in MESADB against BPH and PC

BindingDB (<https://bindingdb.org/rwd/bind/chemsearch/marvin/FMCT.jsp>) tool was used to predict the compound targets and correspondence to known ligand molecules which have minimum similarity of greater than 0.7, and their Gene IDs were retrieved from the UniProtKB (<https://www.uniprot.org>) database. In the same vein, the SMILES of the compounds were uploaded to the Swiss Target Prediction (<http://www.swisstargetprediction.ch/>) database. The study species were humans (*Homo sapiens*) and the probability of each potential target was determined to be >0. Using UniProt, the retrieved targets were converted into standardized abbreviations. Thereafter, the ensuing predicted compound targets from the two databases were pooled together, and this was followed by the removal of duplicates. The GeneCards (<https://www.genecards.org/>) and the DisGeNET databases served as the sources from which disease targets for BPH and PC were obtained. Using the keywords "benign prostatic hyperplasia" and "prostate cancer", the targets from the databases were searched. Next, to avoid occurrence of repeats, the retrieved results were merged. Afterwards, the bioinformatics and evolutionary genomics platform (<https://bioinformatics.psb.ugent.be/webtools/Venn/>) was used to intersect the targets of bioactive compounds of MESADB and disease targets of BPH and PC, following which a Venn diagram was used to represent the common targets of BPH and PC [30].

2.1.3 The construction of protein-protein interaction (PPI) network

To establish the physical connections between cell proteins, we constructed the PPI network of the proteins. The common potential targets were identified from the observed intersections and were uploaded to the database of STRING 11.5 (<https://string-db.org/>). Once PPI network was established, this allowed the interactions between targets to be adequately explored. We had to set the minimum interaction threshold at 0.4, with "*Homo sapiens*" being the species. Following this, was the use of Cytohubba plug-in Cytoscape software (version 3.9.1) to analyze the topology of the network. With the aid of Maximal Clique Centrality (MCC) algorithm, the top 10 key targets were filtered out. The relevant proteins were taken as those which stick closely together in a protein network. The principle of Maximal Clique Centrality (MCC) is that, irrespective of whether low or high-degree proteins, it has a high capacity for capturing important proteins in the top-ranked list [41, 42].

2.1.4 Functions and Pathways of gene enrichment Analysis

Information on the functions of genes such as molecular roles, biological processes and cellular components involved, as well as the crucial pathways associated with biological processes of gene enrichment were obtained using the Gene Ontology (GO) & Kyoto Encyclopedia of Genes and Genomes (KEGG), respectively. This was achieved by submitting the gene IDs of the intersected common targets in the enrichment tool, ShinyGO, version 0.76 (<http://ge-lab.org/go/>), following which analysis was performed with Human as species; false discovery rate (FDR) set at 0.05, and number of pathways = 20 [43].

2.1.5 Molecular docking

A novel component of computational drug design that has emerged in recent years is molecular docking [44]. We further conducted molecular docking analysis to study the strength and mode of interaction between the bioactive compounds from MESADB and the target genes. To achieve binding docking, we used the VINA tool in the PyRx software with a default exhaustiveness of 8. The Protein Data Bank (<https://www.rcsb.org/>) served as the database from which the 3D structures of target genes were retrieved. Also, PubChem (<https://pubchem.ncbi.nlm.nih.gov/>) was the database from which the 3D structures of the bioactive compounds of interest from MESADB were downloaded, after which they were converted to the PDBQT (Protein Data Bank, Partial Charge (Q), and Atom Type (T)) format using Open Babel plug-in in the PyRx software. Ligand energy minimization was achieved via the PyRx software and grid box was maximized to locate the best binding site. This was followed by identification and visualization of the bioactive compounds with the highest binding affinity (kcal/mol) using the Discovery Studio 2021 Client. A docking score of ≤ -5.0 kcal/mol demonstrated by bioactive compounds' interaction and their targets genes represents favorable binding interactions between ligands and receptors [45].

2.2 In vitro studies

2.2.1 Culture of DU-145 Prostate Cancer and Kidney Epithelial Cell Lines (Vero CCL-81)

Human prostate cancer cell line (DU-145) and Kidney epithelial cells (Vero CCL-81), which was the non-cancerous cell used to assess the cellular safety of the MESADB, obtained from the American Type Culture Collection (ATCC) were cultured at the Center for Traditional Medicine and Drug Research (CTMDR), Kenya Medical Research Institute (KEMRI), Nairobi, Kenya. Cell culture was done using Modified Eagle's Medium (MEM, Sigma-Aldrich, USA) as the media, and 1 % L-glutamine (200 mM) (Sigma-Aldrich, USA), 10 % fetal bovine serum (FBS, Gibco, USA), 1.5 % sodium bicarbonate (Loba chemie, India), 1 % HEPES (1 M) (GoldBio, USA), and 1 % penicillin-streptomycin (Sigma-Aldrich, USA), were added as supplements, in a humidified (95% humidity) incubator at 37°C and 5% CO₂. The DU-145 and Vero CCL-81 cell lines used in this research had passage numbers of DU145HTB-81/P-20 and Vero CCL-81/P-15, respectively, and were sub-cultured twice a week. All assays made use of the logarithmic growth phase of the cells. After 80% confluency, the cells were seeded in 96-well plate for MTT (3-(4, 5-dimethylthiazol-2-yl)-2, 5 diphenyltetrazolium bromide) assay [6, 30, 46].

2.2.2 In vitro antiproliferative assessment of MESADB

The (3-(4, 5-dimethylthiazol-2-yl)-2, 5 diphenyltetrazolium bromide) (MTT) assay was adopted to evaluate the antiproliferative/cytotoxic effect of MESADB. On achieving 80 % confluency, the DU-145 cells were washed with phosphate buffered saline (PBS, Sigma-Aldrich, USA) and detached by a 0.25 % trypsin-ethylenediaminetetraacetic acid (trypsin-EDTA) solution (Solarbio, China). Into a sterile Eppendorf tube, was placed 100 μ l of cell suspensions with an addition of 50 μ l of trypan blue (Loba chemie, India) and mixed. Using the hemocytometer, the number of viable cells were counted. Cell suspensions with a cell density of 1×10^4 cells/well were seeded in flat-bottomed 96-well plates and cultured for 24 hours, incubated at 37°C and 5% CO₂. A stock solution of 100,000 μ g/ml of MESADB was prepared initially using 100% dimethyl sulfoxide (DMSO, Finar Chemicals, India), with appropriate dilution using culture medium to achieve a final concentration of 0.2% DMSO in the test sample. Thereafter, the seeding medium was aspirated from the plates. A working concentration of MESADB, 200 μ g/ml (in culture medium) was prepared, from which 100 μ l were added for 48 h as screening treatments. Doxorubicin (Solarbio, China), at equivalent concentration served as the positive control, and 0.2 % DMSO as the negative control. 48 h post exposure of cells to treatments, was followed by addition of 10 μ l of freshly prepared MTT (5 mg/ml) to each well with 4 hours incubation period. Afterwards, MTT was aspirated out, and 100 μ l of 100 % DMSO was added to dissolve the formazan crystals. The absorbance was measured at 570 nm and the 96-well plates were read by Tecan microplate reader (Infinite M1000, Tecan). All assays were conducted in triplicates and percentage of alive cells was calculated by applying the formula below [46, 47].

$$\text{Percentage (\%)} \text{ of alive cells} = (\text{Optical density experimental}) / (\text{Optical density control}) \times 100$$

Following the initial screening at a single concentration (200 μ g/ml), the MESADB with equal or less than 50 % cell survival 48 h post treatment was considered active and subjected to further antiproliferative studies using concentrations ranging from 6.25–200 μ g/ml [48]. This was followed by the determination of the 50 % inhibition concentration (IC₅₀). With the aid of the MTT cell proliferation assay, cytotoxicity of the MESADB was also assessed and 50% cytotoxicity concentration (CC₅₀) determined, using Vero CCL-81 cells.

2.2.3 Selectivity index

In order to determine the selectivity index (SI) for the tested MESADB and doxorubicin, we had to divide the CC_{50} by the corresponding IC_{50} .

2.2.4 Profiling of gene expression

To explore how MESADB causes cytotoxic effect on DU 145 cells, gene expression profiling was conducted according to standard methods [2, 49]. Briefly, using a T-25 flask, 80% of the confluent DU 145 cells were treated with MESADB with equivalent IC_{50} concentration earlier calculated. Non-treated (negative control) cells were exposed to fresh growth media with 0.2% DMSO. Thereafter, cells incubation lasted for 48 hours. This was followed by total RNA extraction, after which reverse transcription was carried out with the aid of FIRE Script RT cDNA synthesis kit (Solis BioDyne, Estonia). For qRT-PCR detection, Luna Universal qPCR Master Mix (New England Biolabs) was used. The primers sequences used (Macrogen Europe BV, Netherlands) are shown in Table 1. The internal reference gene was GAPDH.

Table 1 Primer sequences for RT-qPCR

Gene	Forward Primer	Reverse Primer
PTGS2	GTGCCTGGTCTGATGATGTA	CTGCTTGTCTGGAACAACCTG
EGFR	GTCCAGTATTGATCGGGAGA	TTCCAAATTCCCAAGGACCA
BCL-2	GGCCTCAGGGAACAGAATGAT	TCCTGTTGCTTTTCGTTTCTTTC
GAPDH	CCCCACCACACTGAATCTCC	CTCACCTTGACACAAGCCCA

2.3 Data analysis

Data generated were analyzed using GraphPad Prism version 8.4 software (San Diego, CA, USA), and presented as mean \pm standard error of mean (SEM). One-way Analysis of Variance (ANOVA) followed by Dunnett's post-hoc tests were performed to compare between and across groups. Values were considered statistically significant at p -value < 0.05 .

3 Results

3.1 In silico studies

3.1.1 Identified bioactive compounds present in the MESADB

Table 2 shows the bioactive compounds identified by GC-MS profiling of MESADB, and the chromatogram and structures of the compounds are contained in our previous study [38].

Table 2 The bioactive compounds identified by GC-MS in the MESADB

Peak No	Retention Time (min)	Identity of compound	Peak Area (%)	Molecular Weight (g/mol)	Molecular Formula	Class
1	5.067	Undecane	0.77	156.31	C ₁₁ H ₂₄	Alkanes
2	6.653	2-Pentanol	2.23	88.15	C ₅ H ₁₂ O	Fatty Alcohols
3	9.105	Eicosapentaenoic Acid	1.22	302.5	C ₂₀ H ₃₀ O ₂	Fatty Acids
4	9.233	Shyobunol	1.17	222.37	C ₁₅ H ₂₆ O	Terpenoid
5	9.369	D-Arabinitol	15.71	152.15	C ₅ H ₁₂ O ₅	Carbohydrates
6	9.603	3',5'-Dimethoxyacetophenone	2.44	180.2	C ₁₀ H ₁₂ O ₃	NC
7	9.742	<u>Germacrene D-4-ol</u>	1.11	222.37	C ₁₅ H ₂₆ O	Alcohol
8	10.252	Hexanoic acid, 2-ethylhexyl ester	29.98	228.37	C ₁₄ H ₂₈ O ₂	NC

9	10.34	2,3-Dehydro-4-oxo-7,8-dihydro-.beta.-ionone	2.46	206.28	C ₁₃ H ₁₈ O ₂	NC
10	10.739	Cyclohexanol, 3-ethenyl-3-methyl-2-(1-methylethenyl)-6-(1-methylethyl)-, [1R(1.alpha.,2.beta.,3.alpha.,6.alpha.)]-	0.99	NMW	NMF	NC
11	10.96	9-Oxabicyclo[3.3.1]nonan-2-one,6-hydroxy-	1.4	156.18	C ₈ H ₁₂ O ₃	NC
12	11.409	2,5,9-Tetradecatriene, 3,12-diethyl-	1.06	248.4	C ₁₈ H ₃₂	NC
13	11.566	Solavetivone	1.15	218.33	C ₁₅ H ₂₂ O	Terpenes
14	11.667	Globulol	1.36	222.37	C ₁₅ H ₂₆ O	Terpenoid
15	11.929	2-(1,4,4-Trimethyl-cyclohex-2-enyl)-ethanol	0.48	168.28	C ₁₁ H ₂₀ O	NC
16	12.104	Hexadecanoic acid, methyl ester	2.87	270.5	C ₁₇ H ₃₄ O ₂	Fatty Acids
17	12.15	Eudesma-4(15),7-dien-1.beta.-ol	0.69	220.35	C ₁₅ H ₂₄ O	Terpenoids
18	12.232	Platambin	1.22	238.37	C ₁₅ H ₂₆ O ₂	Terpenoids
19	12.416	Pentadecanoic acid	3.77	242.4	C ₁₅ H ₃₀ O ₂	Fatty Acids
20	12.562	Glyceryl diacetate 2-linolenate	1.47	436.6	C ₂₅ H ₄₀ O ₆	NC
21	12.923	Cyclopropane, 1-(1-hydroxy-1-heptyl)-2-methylene-3-pentyl-	0.63	238.41	C ₁₆ H ₃₀ O	NC
22	13.396	9,12-Octadecadienoic acid, methyl ester	6.64	294.5	C ₁₉ H ₃₄ O ₂	Fatty Acids
23	13.426	9-Octadecenoic acid (Z)-, methyl ester	2.51	296.5	C ₁₉ H ₃₆ O ₂	Fatty Acids
24	13.458	Methyl linolenate	1.69	292.5	C ₁₉ H ₃₂ O ₂	Fatty Acids
25	13.499	Phytol	1	296.5	C ₂₀ H ₄₀ O	Fatty Acids
26	13.525	Methyl 2-nonynoate	0.86	168.23	C ₁₀ H ₁₆ O ₂	Fatty Acids
27	13.595	Methyl stearate	0.93	298.5	C ₁₉ H ₃₈ O ₂	Fatty Acids
28	13.97	Tricyclo[20.8.0.0(7,16)]triacontane, 1(22),7(16)-diepoxy-	1.57	444.7	C ₃₀ H ₅₂ O ₂	Fatty acids
29	16.624	2-Palmitoylglycerol	1.2	330.5	C ₁₉ H ₃₈ O ₄	Glycerides
30	18.052	Glyceryl monolinoleate	3.02	354.5	C ₂₁ H ₃₈ O ₄	Glycerides
31	22.287	beta.-Tocopherol	0.84	416.7	C ₂₈ H ₄₈ O ₂	Vitamin
32	24.929	Benzenepropanoic acid, .alpha.-(1-hydroxyethyl)-.beta.-phenyl-	5.59	270.32	C ₁₇ H ₁₈ O ₃	NC

NMW=No Molecular Weight, NMF=No Molecular Formula, NC=Not Classified

3.2 Prediction of physicochemical properties of drug candidates using Swiss ADME Tool

Table 3 shows the detailed results of the drug candidates screening of 31 of the 32 compounds identified in the MESADB as one of the compounds (M10) did not successfully go through the screening. Out of the 31 compounds, only three (3) were considered ideal drug-like candidates which include Undecane, D-Arabinitol, and 9-Oxabicyclo [3.3.1] nonan-2-one,6-hydroxy- (Table 4).

Table 3 Prediction of Drug-likeness of MESADB using ADME profiles

Ligands Number	Physical and chemical properties						Lipinski Violations	Veber Violations	Egan Violations	Ghose Violations	Muegge Violations	BBB
	MW (g/mol)	Molar refractive index	Rotatable bonds number	LogP (Octanol/Water)	H-bond Acceptors Number	H-bonds donors Number						
Threshold	≤500	40≤MR≤130	≤10	≤5	≤10	≤5	Yes/No	Yes/No	Yes/No	Yes/No	Yes/No	Yes/No
M1*	156.31	54.99	8	5.11	0	0	YES,1	YES, 0	YES, 0	NO, 1	NO, 3	NO
M2	88.15	27.31	2	1.16	1	1	YES, 0	YES, 0	YES, 0	NO, 3	NO, 2	YES
M3	302.45	97.66	13	4.67	2	1	YES, 1	NO, 1	NO, 1	NO, 1	NO, 1	NO
M4	222.37	72.06	3	3.56	1	1	YES, 0	YES, 0	YES, 0	YES, 0	NO, 1	YES
M5*	152.15	31.96	4	-2.33	5	5	YES, 0	YES, 0	YES, 0	NO, 3	NO, 2	NO
M6	180.2	49.62	3	1.13	3	0	YES, 0	YES, 0	YES, 0	YES, 0	NO, 1	YES
M7	222.37	72.36	1	3.56	1	1	YES, 0	YES, 0	YES, 0	YES, 0	NO, 1	YES
M8	228.37	70.7	11	3.69	2	0	YES, 0	NO, 1	YES, 0	YES, 0	YES, 0	YES
M9	206.28	61.68	3	1.93	2	0	YES, 0	YES, 0	YES, 0	YES, 0	YES, 0	YES
M10	NIL											
M11*	156.18	38.79	0	-0.12	3	1	YES, 0	YES, 0	YES, 0	NO, 2	NO, 1	NO
M12	248.45	87.22	10	5.66	0	0	YES, 0	YES, 0	NO, 1	NO, 1	NO, 2	NO
M13	218.33	68.98	1	3.46	1	0	YES, 1	YES, 0	YES, 0	YES, 0	NO, 1	YES
M14	222.37	68.82	0	3.81	1	1	YES, 0	YES, 0	YES, 0	YES, 0	NO, 1	YES
M15	168.28	53.04	2	2.59	1	1	YES, 0	YES, 0	YES, 0	YES, 0	NO, 2	YES
M16	270.45	85.12	15	4.44	2	0	YES, 0	NO, 1	YES, 0	NO, 1	NO, 1	YES

M17	220.35	69.94	1	3.56	1	1	YES, 1	YES, 0	YES, 0	YES, 0	NO, 1	YES
M18	238.37	71.58	1	2.74	2	2	YES, 0	YES, 0	YES, 0	YES, 0	YES, 0	YES
M19	242.4	75.99	13	3.94	2	1	YES, 0	NO, 1	YES, 0	YES, 0	NO, 1	YES
M20	436.58	124.72	21	4	6	0	YES, 0	NO, 1	YES, 0	NO, 2	NO, 2	NO
M21	248.45	87.22	10	5.66	0	0	YES, 0	YES, 0	NO, 1	NO, 1	NO, 2	NO
M22	218.33	68.98	1	3.46	1	0	YES, 1	YES, 0	YES, 0	YES, 0	NO, 1	YES
M23	222.37	68.82	0	3.81	1	1	YES, 0	YES, 0	YES, 0	YES, 0	NO, 1	YES
M24	168.28	53.04	2	2.59	1	1	YES, 0	YES, 0	YES, 0	YES, 0	NO, 2	YES
M25	270.45	85.12	15	4.44	2	0	YES, 0	NO, 1	YES, 0	NO, 1	NO, 1	YES
M26	220.35	69.94	1	3.56	1	1	YES, 1	YES, 0	YES, 0	YES, 0	NO, 1	YES
M27	238.37	71.58	1	2.74	2	2	YES, 0	YES, 0	YES, 0	YES, 0	YES, 0	YES
M28	444.73	138.08	0	6.14	2	0	YES, 1	NO, 1	YES, 0	NO, 1	NO, 1	NO
M29	330.5	97.06	18	6.14	4	2	YES, 0	YES, 0	NO, 1	YES, 0	NO, 1	YES
M30	354.52	105.72	18	3.42	4	2	YES, 0	NO, 1	YES, 0	YES, 0	NO, 2	YES
M31	416.68	134.31	12	5.94	2	1	YES, 1	NO, 1	NO, 1	NO, 1	NO, 1	NO
M32	270.32	78.06	5	3.01	3	2	YES, 0	YES, 0	YES, 0	YES, 0	YES, 0	YES

*Compound M10 had no information

Table 4 Prediction of ADMET *in silico* pharmacokinetic profiles of Ideal drug-like candidates selected from bioactive compounds of MESADB

Compounds number	Absorption	Distribution		Metabolism							Excretion	Toxicity			
	Intestinal Absorption (Human)	Permeability		Substrate		Inhibitor					Total Excretion				
		BBB	CNS	2D6	3A4	1A2	2C19	2C9	2D6	3A4					
	Numeric (% Absorbed)	Numeric (log BB)	Numeric (Log PS)	Categorical (Yes/No)							Numeric (Log ml/min/kg)	Categorical (Yes/No)			
M1	92.764	0.844	-1.69	NO	NO	NO	NO	NO	NO	NO	NO	1.654	M1	92.764	0.844
M5	29.627	-1.153	-4.028	NO	NO	NO	NO	NO	NO	NO	NO	0.859	NO	NO	NO
M11	96.549	-0.285	-3.267	NO	NO	NO	NO	NO	NO	NO	NO	1.269	NO	NO	NO

3.2.1 Identification of Overlap Targets among Drug Candidates of MESADB, BPH & PC

A total of 141 potential targets were identified as targets for the 3 prioritized bioactive compounds of the MESADB, using the SWISS Target Prediction (STP) and BindingDB (BDB) databases following removal of duplicates. Furthermore, a total of 1967 target genes that are closely related to BPH and PC after removal of duplicates were retrieved and retained from the GeneCards and DisGeNET databases. The gene data sets obtained from the 141 related targets of MESADB, and the 1967 BPH and PC related targets overlapped, and a total of 56 intersecting gene targets were obtained which were represented into an online Venn diagram (Figure 1).

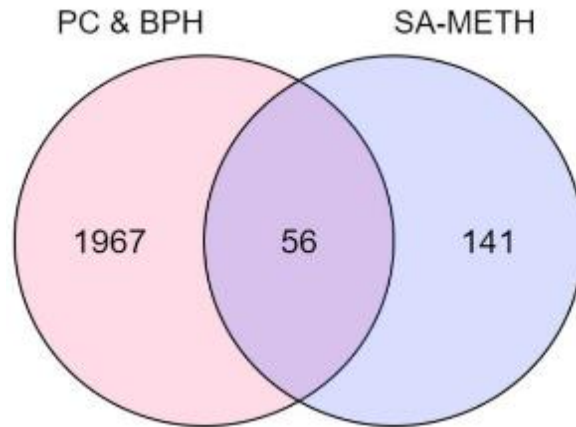


Figure 1 Identification of Overlap Targets among Drug Candidates of MESADB (SA-METH), BPH and Pc

3.2.2 Construction of Compound-BPH-PC Protein-Protein Interaction (PPI) network

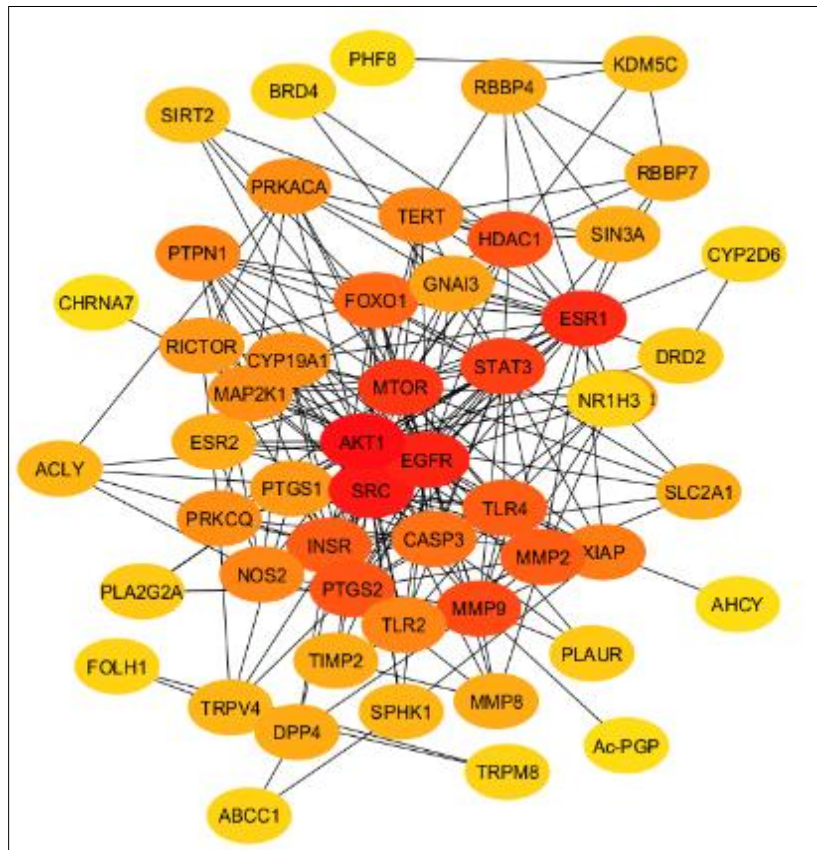


Figure 2 PPI interaction network of 56 potential anti-PC/BPH targets of MESADBP constructed using STRING Database. The red colour intensity indicates the significance of the target genes in the PPI network

A total of 56 key target genes were obtained by mapping the targets of the compounds from the MESADB to the BPH and PC disease targets. The 56 targets were imported into the STRING database, retrieved in TSV format, and imported into Cytoscape for visualization and analysis which led to the retrieval of a network consisting of 56 nodes and 263 edges (Figure 2). The average node degree was 9.39, the average local clustering coefficient was 0.555, and the PPI enrichment p-value was $< 1.0e-16$, which implies that proteins have more interactions among themselves than would be expected for a random set of proteins of similar size drawn from the genome. Thereafter, the top 10 hub targets of selected drug candidates of MESADB were obtained (Figure 3).

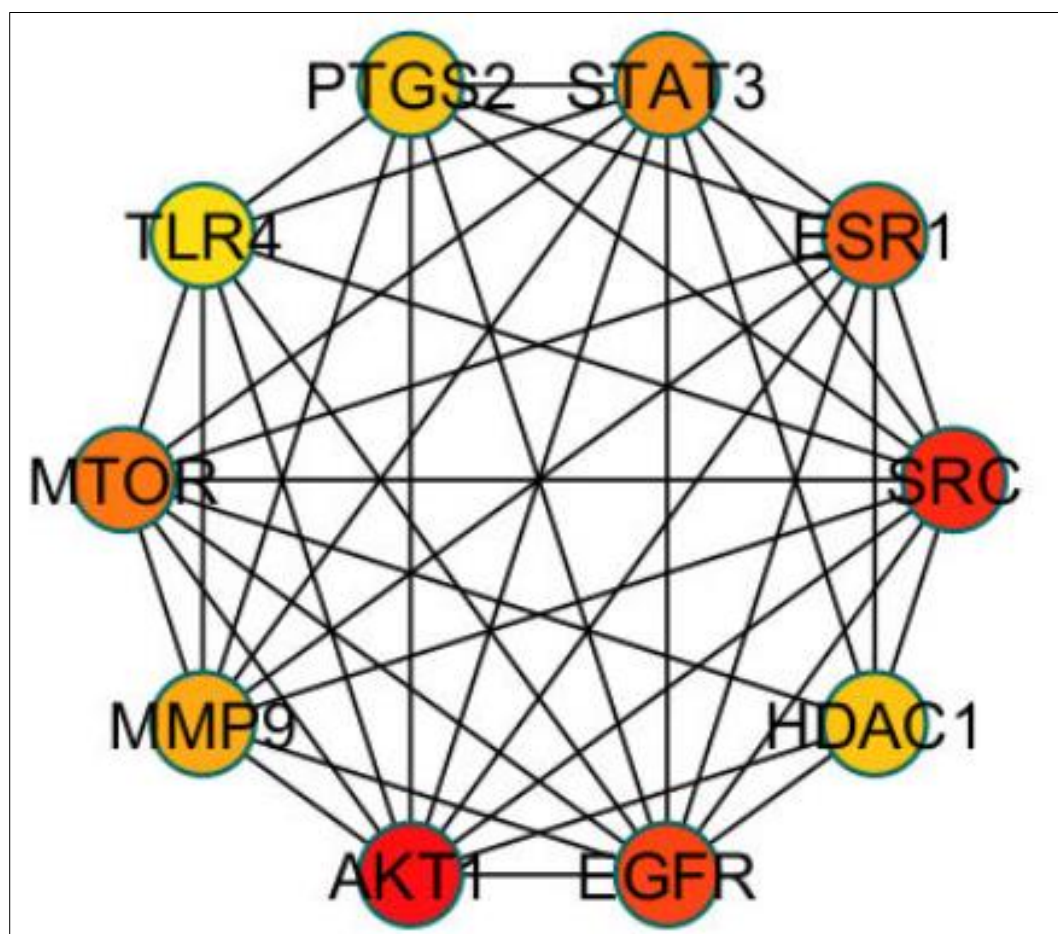


Figure 3 PPI network for the top 10 hub targets for MESADB. The intensity of the colour represents the significance ($p < 0.05$) of the targets, with darker red indicating a higher degree.

3.2.3 Combination of Overlap Targets among Drug Candidates, BPH & PC; Construction of Compound-BPH-PC PPI network and Top-10-hub-targets

Figure 4 shows the intersection of the potential proteins of bioactive compounds from MESADB and disease targets of prostate cancer (PC) and benign prostatic hyperplasia (BPH), protein-protein interaction (PPI) network and top 10 hub target genes [A, Venn diagram of overlap targets; B, PPI network of targets of MESADB, and PC & BPH; C, top 10 core targets of MESADB].

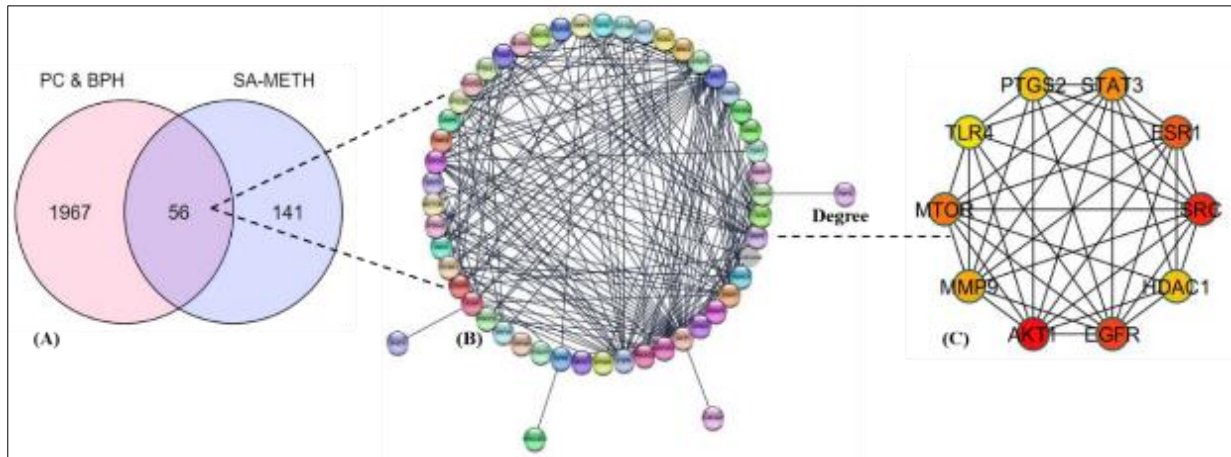


Figure 4 MESADB(SA-METH) -PC & BPH intersection., PPI network and top 10 hub target genes

3.2.4 Gene Ontology enrichment terms of MESADB

The 56 key targets of the bioactive compounds from MESADB against BPH and PC were enriched in 678 GO (Gene Ontology) including 601 for biological processes (BP) terms, 53 for molecular function (MF) terms and 24 for cellular components (CC) terms ($p < 0.05$). In the dot plot charts, the top significant GO terms for each category were represented (Figures 5-7). Their order of relevance were ranked from top to bottom using $-\log_{10}$ (p value). The GO analysis demonstrated that the key targets are involved in the biological processes (BP) with roles including response to oxygen containing compound, response to hormone, regulation of cell population proliferation, inflammatory response, and regulation of cell death. The cellular components (CC) were mainly enriched in the membrane raft, membrane micro domain and cell surface. There was association of key targets with various molecular functions through Molecular function (MF) analysis including nuclear receptor activity, zinc ion binding, ligand-activated transcription factor activity, transition metal ion binding and steroid binding. It was revealed by the Kyoto Encyclopedia of Genes and Genomes (KEGG) pathway analysis that the key targets were significantly enriched in 123 pathways, and by $-\log_{10}$ p values (Figure 8), the top 20 significant pathways were screened which gave rise to selection of the top 10 KEGG pathways that were subjected to analysis as the most important molecular pathways involved in the actions of the bioactive compounds from the MESADB against BPH and PC (Table 5).

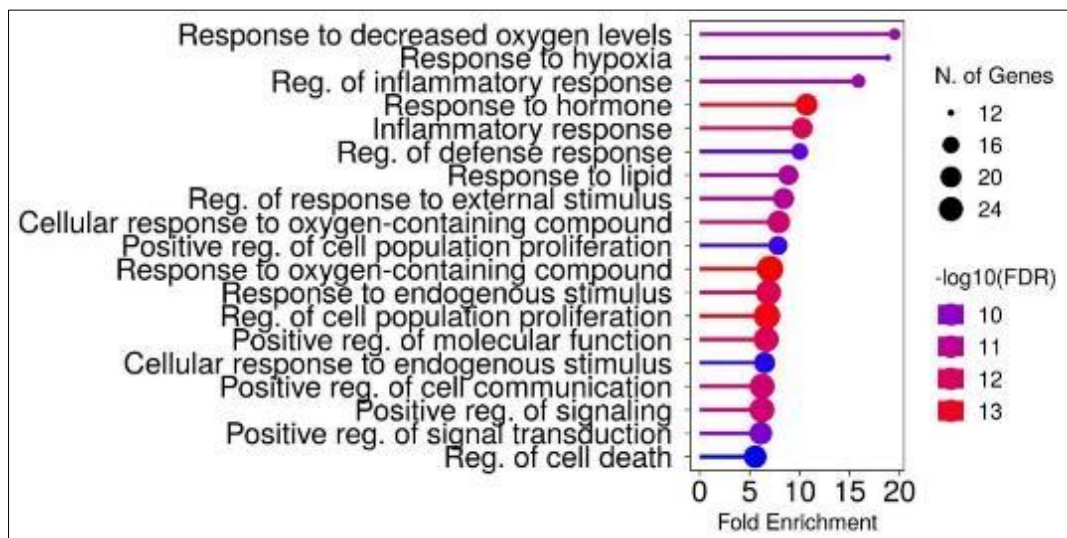


Figure 5 Biological processes of Gene Ontology enrichment terms of MESADB in PC & BPH. The y-axis represents the enriched categories, the x-axis represents the number of enrichments, the colour explains the importance of pathways using FDR by $-\log_{10}$ (p value), the higher the FDR, the more significant.

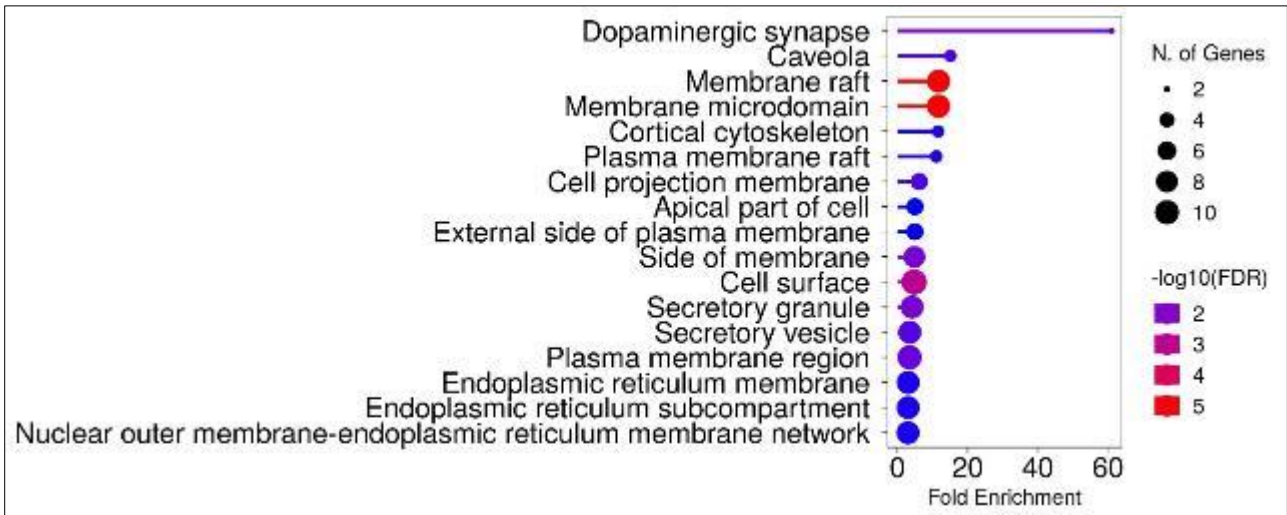


Figure 6 Cellular components of Gene Ontology enrichment terms of MESADB in PC & BPH. The y-axis represents the enriched categories, the x-axis represents the number of enrichments, the colour explains the importance of pathways using FDR by $-\text{Log}_{10}$ (p value), the higher the FDR, the more significant.

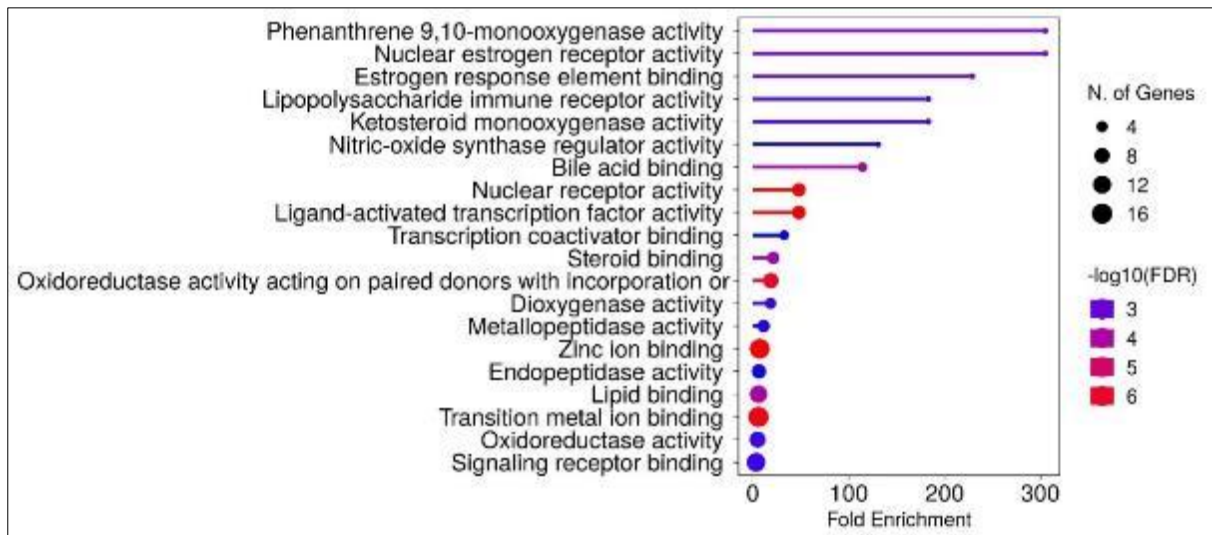


Figure 7 Molecular function terms of Gene Ontology enrichment terms of MESADB in PC & BPH. The y-axis represents the enriched categories, the x-axis represents the number of enrichments, the colour explains the importance of pathways using FDR by $-\text{Log}_{10}$ (p value), the higher the FDR, the more significant.

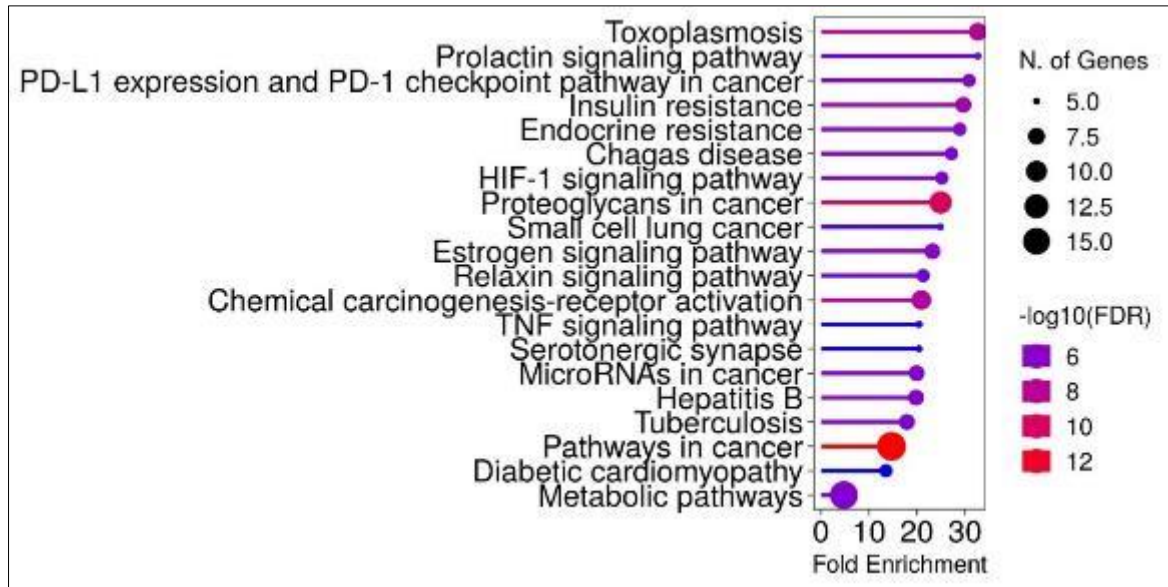
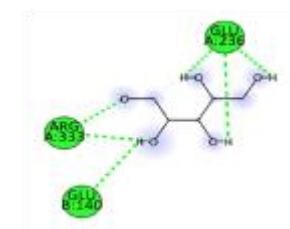
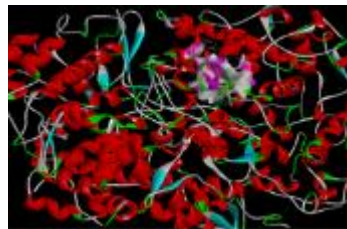
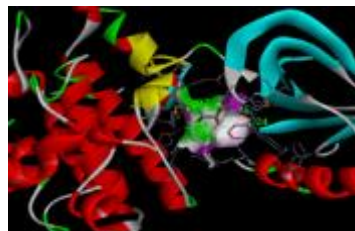


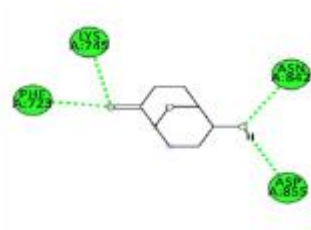
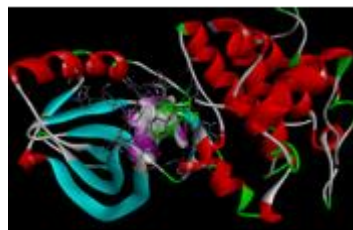
Figure 8 KEGG enrichment pathways of MESADB in PC & BPH. The y-axis represents the enriched categories, the x-axis represents the number of enrichments, the colour explains the importance of pathways using FDR by $-\log_{10}$ (p value), the higher the FDR, the more significant.



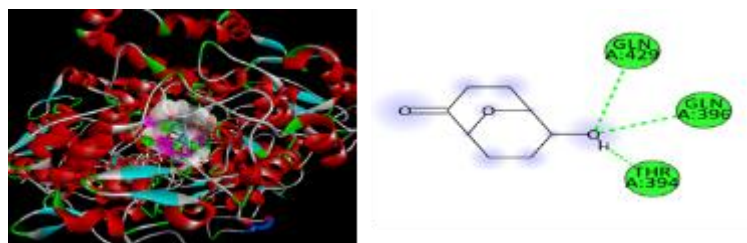
D-Arabinitol (M5) -PTGS2 complex



D-Arabinitol (M5) -EGFR complex



9-Oxabicyclo [3.3.1] nonan-2-one, 6-hydroxy (M11) -EGFR complex



9-Oxabicyclo [3.3.1] nonan-2-one, 6-hydroxy (M11)-PTGS2 complex

Keys

Interactions



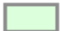



	Conventional Hydrogen Bond		Pi-Sigma
	Carbon Hydrogen Bond		Pi-Pi Stacked
	Pi-Cation		Pi-Alkyl

Figure 9 3D and 2D representation of the interactions of the selected drug candidates from the bioactive compounds from the MESADB with PC & BPH

Table 5 Top 10 enriched KEGG pathways of MESADB targets in PC & BPH (the order of importance was ranked from top to bottom by $-\text{Log}_{10}$ (p value))

Score	Pathways	P-value	Gene count
1	Path: hsa05200 Pathways in cancer	1.24E-13	17
2	Path: hsa05205 Proteoglycans in cancer	5.50E-11	11
3	Path: hsa05145 Toxoplasmosis	7.95E-09	8
4	Path: hsa05207 Chemical carcinogenesis-receptor activation	2.06E-08	9
5	Path: hsa04931 Insulin resistance	1.49E-07	7
6	Path: hsa04915 Estrogen signaling pathway	6.88E-07	7
7	Path: hsa05235 PD-L1 expression and PD-1 checkpoint pathway in cancer	1.19E-06	6
8	Path: hsa01522 Endocrine resistance	1.25E-06	6
9	Path: hsa05161 Hepatitis B	1.25E-06	7
10	Path: hsa05206 MicroRNAs in cancer	1.25E-06	7

3.2.5 Molecular Docking

We selected top 10 hub target proteins for molecular docking to further investigate the interactions between the bioactive compounds from MESADB and their target genes. The structures of the compounds [Undecane, D-Arabinitol, and 9-Oxabicyclo [3.3.1]nonan-2-one,6-hydroxy-] were uploaded to VINA tool of the PyRx software for analysis of their potentials for docking with TLR4, PTGS2, STAT3, ESR1, MTOR, SRC, MMP9, HDAC1, AKT1, and EGFR. The three selected bioactive compounds were each docked separately with the top 10 hub target genes, after which the docking score for each target protein was recorded (Table 6). A docking score of -5.0 kcal/mol or less is indicative of a favorable binding interactions between ligands and receptors in accordance with the VINA scoring system [45]. To this end, the molecular docking analysis showed a significant binding affinity of two of the compounds (M5 and M11) from the MESADB with their target genes. A strong docking activity was demonstrated between these compounds and two hub target genes, PTGS2 and EGFR as seen in the respective docking scores of below -5.0 kcal/mol (Table 6). This, therefore, infers a high level of accuracy in the process of selection of the top 10 hub target genes as well as pointing towards potential effectiveness of these bioactive compounds in BPH and PC treatment. The 3D and 2D interactions of the selected drug candidates from the bioactive compounds of the MESADB with target genes of BPH & PC are shown (Figure 9).

Table 6 Binding affinities and ligand-receptor interactions of selected drug candidates from bioactive compounds of MESADB with selected hub genes.

Complex	Binding energy (kcal/mol)	Interaction residues	Type of bond
M5-PTGS2	-5.1	Glu140, Arg333, Glu236	Hydrogen
M5-EGFR	-5.4	Kxy1103, Asp837, Tyr869, Asn842, Arg841	Hydrogen
M11-PTGS2	-5.7	Gln429, Glu396, Thr394	Hydrogen
M11-EGFR	-5.8	Phe723, Lys745, Asn842, Asp855	Hydrogen

3.3 In vitro studies

3.3.1 In vitro antiproliferative assessment of MESADB

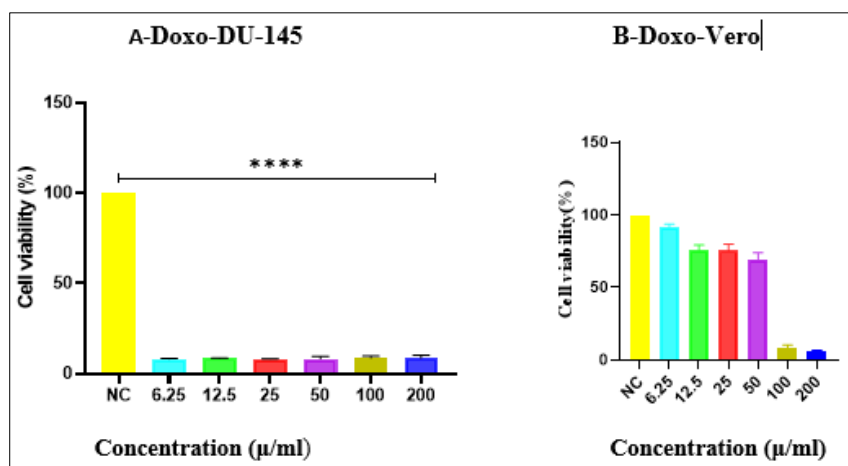
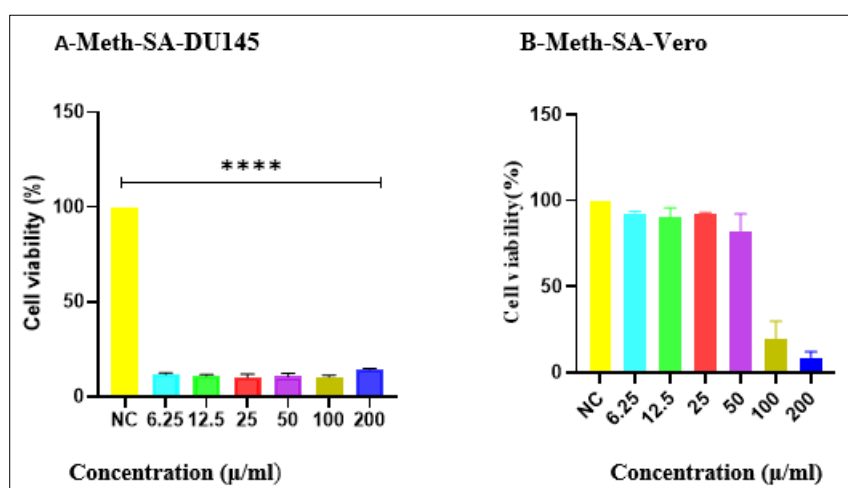


Figure 10 (A) Inhibition of cellular proliferation by Doxorubicin (Positive Control): Inhibition of cellular proliferation on serial concentrations 2-fold dilution on DU-145 cells to obtain IC_{50} of Doxorubicin, NC= Negative Control (0.2% of DMSO) (B). Cellular safety: Determination of cellular safety of doxorubicin using kidney epithelial non-cancerous Vero CCL-81, at 2-fold serial dilution of the doxorubicin to determine CC_{50} .

All treatments lasted for 48 h and were done in triplicate ($n = 3$); values were expressed as Mean \pm SEM, Significant at $p \leq 0.05$; **** $p \leq 0.0001$.



All treatments lasted for 48 h and were done in triplicate ($n = 3$); values were expressed as Mean \pm SEM, Significant at $p \leq 0.05$; **** $p \leq 0.0001$.

Figure 11 (A) Inhibition of cellular proliferation by MESADB: Inhibition of cellular proliferation on serial concentrations 2-fold dilution on DU-145 cells to obtain IC_{50} of MESADB, NC= Negative Control (0.2% of DMSO) (B). Cellular safety: Determination of cellular safety of MESADB using kidney epithelial non-cancerous Vero CCL-81, at 2-fold serial dilution of the MESADB to determine CC_{50} .

3.3.2 Selectivity index (SI)

The IC₅₀ and CC₅₀ values for doxorubicin and MESADB were obtained from the data in figures 10 and 11, respectively. The IC₅₀ and CC₅₀ of MESADB were 5.11 µg/ml and 75.833 µg/ml respectively, which gave a calculated SI of 14.84. whereas the IC₅₀ and CC₅₀ values of doxorubicin were 4.643 µg/ml and 53.210µg/ml, resulting to a calculated SI of 11.46.

3.3.3 Gene expression analysis

The mRNA expression of EGFR, PTGS2 and BCL-2 were determined by RT-qPCR to validate the top putative molecular targets of MESADB in DU-145 prostate cancer cells as demonstrated by network pharmacology and molecular docking (Figure 3, Table 6). EGFR and PTGS2 were among the top ten target genes which also showed strong docking activities with the promising compounds of MESADB. In addition, we included the BCL-2 gene owing to its function in cell proliferation and apoptosis. The relative mRNA expression levels of target genes were normalized to GAPDH as the housekeeping gene using the 2^{-ΔΔCt} method. The results are presented in Fig. 12. There were significant downregulation of EGFR ($p < 0.0001$), PTGS2 ($p < 0.0001$), and BCL-2 ($p < 0.0001$), compared to untreated control.

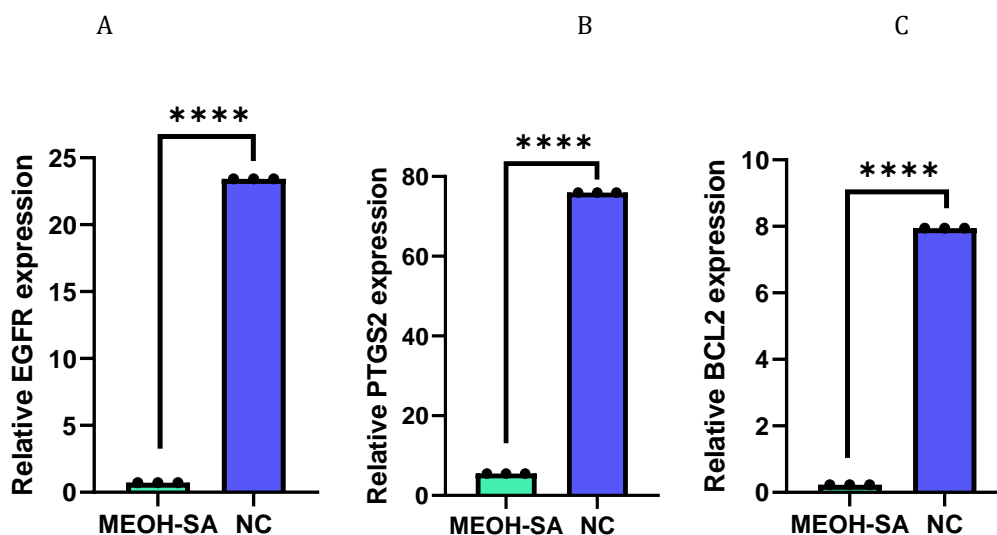


Figure 12 Relative gene expression analysis of MESADB treated DU-145 cells and the untreated control (0.2 % DMSO). (A) EGFR, (B)PTGS2, (C) BCL-2. **** $p \leq 0.0001$ as compared to untreated control

4 Discussion

The current study focused on evaluation of the potentials of GC-MS identified bioactive compounds from the MESADB against BPH and PC through network pharmacological and *in vitro* experimental approach. Using the Rule of 5 (RO5) that incorporates evaluation of the pharmacokinetic profiles of drug candidates such as absorption, distribution, metabolism, and excretion (ADME), the blood-brain barrier, liver drug metabolizing enzymes including CYP2D6 and CYP3A4, as well as the toxicity profiles (ADMET), 3 bioactive compounds with promising drug-likeness properties were identified out of the GC-MS identified bioactive compounds from the MESADB. A total of 56 common potential target proteins of the selected bioactive compounds, BPH and PC were identified. Of these, the top 10 hub targets with better protein-protein-interaction (PPI) network were selected including TLR4, PTGS2, STAT3, ESR1, MTOR, SRC, MMP9, HDAC1, AKT1 and EGFR, which represent potential targets of the bioactive compounds from MESADB against BPH and PC.

Our results of the protein-protein interaction (PPI) network construction revealed 56 nodes, 263 edges, average node degree of 9.39, average local clustering coefficient of 0.555, and PPI enrichment p-value of less than 1.0e-16. This therefore suggests that the proteins have good interactions within the network. The edges represent the strings linking the proteins and the 263 edges in our study represent a better interaction amongst the proteins since there are more links connecting the proteins. This means that a particular protein with more links to various other proteins in the network may activate or deactivate other connected proteins, therefore suggesting that proteins work as a cluster within the network. The number of nodes reflects the number of genes earlier loaded in the STRING database. The node degree is obtained through the number of edges or linkages one protein has with others and the more the linkages with other proteins, the more the node degree. Therefore, in our study, an average node degree of 9.39 was obtained meaning

that the top 10 selected hub genes had more connections, hence more interactions with various other proteins, for which reason they were selected. The cluster coefficient in PPI is the measure of the degree to which the proteins cluster together and represents the interconnectivity of the proteins within the network. It broadens understanding of the biological network amongst a group of proteins which work together to achieve a specific biological function.

Several studies have reported the involvement of the identified top 10 genes in benign prostatic hyperplasia (BPH) and prostate cancer (PC). The presence of the epidermal growth factor (EGF) and its receptor (EGFR) was revealed in samples of human benign prostatic hyperplastic patients [50]. Furthermore, a retrospective study which examined normal prostates, benign hyperplastic and neoplastic prostatic tissues for the presence of a variant EGFR (EGFRvIII) revealed the progressive increase in the expression of this mutant receptor with a gradual transformation of the tissues to the malignant phenotype which may explain the role of this receptor in the occurrence and progression of prostate cancer, further suggesting it, as a possible target in prostate cancer therapy [51]. Similarly, the AKT Serine/Threonine Kinase 1 (AKT-1) gene has also been implicated in BPH and PC patients [52, 53]. This suggests AKT-1 as a potential target for BPH and PC.

The Matrix metalloproteinases (MMPs) family have proteolytic effects on cell membranes; and MMP9 is specifically known to release proangiogenic factors which exerts its effects on endothelial cells, provoking cell migration and proliferation. An elevated level of MMP9 results to metastasis in androgen-independent prostate cancer [54]. Prostaglandin endoperoxide synthase 2 (PTGS2) is known to catalyze the rate-limiting step in the synthesis of prostaglandins which are potent inflammatory mediators, whose expression is controlled by cytokines, growth factors, and tumour promoters [55]. Studies have reported the significant roles of PTGS2 gene in suppression of the immune system, apoptosis, cell proliferation, tumour progression and metastasis [56, 57], and has been implicated in a number of cancers including prostate cancer (PC) [58–61].

Furthermore, signal transducer and activator of transcription 3 (STAT3) has also been implicated in prostate cancer. The findings from a previous study revealed that the activation of the STAT3 signaling pathway was involved in prostate cancer cell growth that was stimulated by interleukin-6 (IL-6) expression [62]. The *Estrogen Receptor 1* (ESR1) has been implicated in benign prostatic hyperplasia, metastatic and non-metastatic prostate cancer [63], which is also consistent with the reports that ESR1 expression caused permanent enlargement of the prostate gland and escalated androgen responsiveness [64], making it a spotlight target for therapeutic interventions of these conditions. The involvement of the mammalian target of rapamycin (mTOR) signaling pathway on the protective effect of interleukin 8 (IL-8) on prostate cancer cells has been revealed. It was reported in a study which demonstrated the effect of GSK-3 β in inducing oxidative stress to cause prostate cancer cell death, that interleukin-8 (IL-8) protects the prostate cancer cells via activation of the mTOR signaling pathway, leading to the attenuation of oxidative stress through inhibition of GSK-3 β [65].

Certain group of proteins referred to as activators or repressors which are said to be co-regulators interacting with nuclear receptors have been shown to be part of the androgen receptor (AR) activation process. These co-regulators could alter the transactivation of the nuclear receptors leading to enhancement of events such as remodeling of chromatin, recruitment of pre-initiation complex and movement of RNA polymerase [66, 67]. The nuclear receptor co-activator 1 (NCOA1), also known as steroid receptor co-activator-1 (SRC1), nuclear receptor co-activator 2 (NCOA2) or steroid receptor co-activator-2 (SRC2) and nuclear receptor co-activator 3 (NCOA3) or steroid receptor co-activator-3 (SRC3), all belonging to the p160/SRC *proto-oncogene tyrosine-protein kinases* protein family, are among the most studied co-activator groups with such co-regulatory functions [68]. Investigations have demonstrated that AR co-regulators alteration could play a role in prostate cancer progression [66, 67], as elevated expression of SRC1 was seen in prostate tumours [69]. In addition, the SRCs are known for their important functions in diverse cellular processes such as cell motility, morphology, proliferation and survival [70].

The toll-like receptor (TLR) family, include a group of proteins involved in pathogen recognition with innate immunity and play important roles in the immunity process of pathogens [71–73]. The toll-like receptor-4 (TLR4) has been linked with the risk of occurrence of benign prostatic hyperplasia (BPH) and prostate cancer (PC). Studies have demonstrated that TLR4 may trigger the induction of T cells differentiation, causing generation of cytokines, and may also mediate inflammatory responses through Nuclear factor kappa B (NF- κ B) signaling, in a bid to building adaptive immunity [74–76]. It was demonstrated in a study conducted among Chinese population that mutation in TLR4 which disrupts its normal functioning could pose a risk and poor prognosis of BPH [77]. Furthermore, activation of TLR4 by Gram-negative bacteria lipopolysaccharide (LPS) provokes cascades of inflammatory reactions that leads to production of cytokines, making LPS an agonist of TLR4 [78]. Frequent exposure to LPS has been shown to promote progression and metastasis of prostate cancer [79], therefore pointing out the possibility of bacterial infection or TLR4 stimulation by LPS in the pathogenesis of prostate cancer [80].

Histone deacetylase 1 (HDAC1) is a co-repressor that controls cell differentiation and proliferation, eliciting its function by targeting p53 amongst other transcription factors, mostly elevated in malignant tissues such as in prostate cancer, though could also be expressed in benign tissues such as in benign prostatic hyperplasia at a lower level [81, 82], and has been associated with the development of prostate cancer [83]. As obvious, the identified top 10 hub target genes play significant roles in benign prostatic hyperplasia (BPH) and prostate cancer (PC), putting them in a spotlight as potential targets for the therapeutic interventions of these prostatic conditions.

We conducted Gene Ontology (GO) analysis to investigate the molecular functions of the genes, biological processes and cellular components involved in the actions of the bioactive compounds of the MESADB. The GO analysis revealed different crucial biological processes such as response to oxygen containing compound, response to hormone, regulation of cell population proliferation, inflammatory response, and regulation of cell death. The cellular components (CC) were mainly enriched in the membrane raft, membrane micro domain and cell surface. There was association of key targets with various molecular functions (MF) including nuclear receptor activity, zinc ion binding, ligand-activated transcription factor activity, transition metal ion binding and steroid binding. The KEGG pathway analysis which was conducted to identify the possible significant pathways through which the bioactive compounds of the MESADB may act revealed pathways in cancer, pathway of proteoglycans in cancer, pathways in toxoplasmosis, chemical carcinogenesis-receptor activation pathways, pathways in insulin resistance, estrogen signaling pathway, PD-L1 expression and PD-1 checkpoint pathway in cancer, pathways in endocrine resistance, Hepatitis B pathway, and MicroRNAs in cancer pathways.

Molecular docking is an important aspect of network pharmacology that enhances the validity and accuracy of the *in silico* evaluation results [84, 85]. Our molecular docking results revealed that the bioactive compounds from MESADB which earlier showed their drug-like properties and sailed through the screening process demonstrated good docking activities with high binding affinity with two core target proteins (PTGS2 and EGFR), which further strengthens the prediction of the compounds' therapeutic potentials against BPH and PC. To further validate the results obtained from network pharmacology prediction, we conducted *in vitro* antiproliferative and gene expression analysis. Interestingly, our results on anti-proliferative assay revealed that MESADB caused significant anti-proliferative effects on the DU-145 prostate cancer cell lines while sparing the non-cancerous kidney epithelial cells (Vero CCL-81). The IC₅₀ value with which MESADB demonstrated selective cytotoxic activities against DU-145 cells was 5.11 µg/ml. Doxorubicin, which was the standard positive control drug used, caused cytotoxicity against DU-145 cells with an IC₅₀ value of 4.643 µg/ml, which was at a close range with that of MESADB. The CC₅₀ value of MESADB on Vero CCL-81 cells was 75.833 µg/ml, implying relatively non-cytotoxic effects on Vero cells. Also, doxorubicin had a CC₅₀ of 53.210 µg/ml on Vero cells. The resultant selectivity index (SI) of MESADB was 14.84. while doxorubicin had an SI of 11.46.

Furthermore, to validate the predicted molecular targets of MESADB in BPH and PC, we conducted gene expression analysis using RT-qPCR. Previous study reported increased expression of a variant EGFR (EGFRvIII) in BPH and PC [51]. Treatment of DU-145 with MESADB showed a significant downregulation of EGFR compared to control. This result further supports the outcome of our molecular docking analysis and gives credence to the anti-proliferative assays. Studies have revealed the role of PTGS2 gene in suppressing the immune system, apoptosis, cell proliferation, tumour progression and metastasis [56, 57], and it being implicated in a number of cancers including prostate cancer (PC) [58–61]. Our analysis showed a significant downregulation of PTGS2 gene in treated DU-145 prostate cancer cells compared to untreated control, supporting our *in silico* molecular docking findings as well as anti-proliferative assays. BCL-2 is an anti-apoptotic gene, involved in the control of mitochondrial apoptotic pathway through mechanisms involving binding to pro-apoptotic proteins, prevention of pore formation and release of cytochrome C [30]. In our study, there was a significant downregulation of BCL-2 gene in treated DU-145 prostate cancer cells compared to untreated control, again supporting the potential role of our MESADB in treatment of BPH and PC.

According to one of the criteria for a plant extract or fraction to be considered for purification as a promising therapeutic drug agent, it should possess an IC₅₀ < 30 µg/ml, as established by the US National Cancer Institute (NCI) [86]. Therefore, based on this criterion, MESADB showed promising result. With the understanding that drugs with low IC₅₀ values are likely to be effective at low concentrations, which may translate to reduced risk of systemic untoward effects when taken [30], the low IC₅₀ value observed with MESADB and selective cytotoxic activities against DU-145 prostate cancer cells suggest this plant as a potential source for drug candidates against prostatic conditions such as prostate cancer (PC) and benign prostatic hyperplasia (BPH).

The findings from our study partly conform and partly differ from the outcome of a previous study which evaluated the anti-proliferative activities of methanol extract and diethyl ether, chloroform and aqueous fractions of *S. aculeastrum* Dunal berries (SADB) against various cancerous cell lines including A2780 (ovarian carcinoma), Caco-2 (colon carcinoma), DU-145 (prostate carcinoma), HepG2 (hepatocarcinoma), MCF-7 (breast carcinoma), MDA-MB-231 (breast

adenocarcinoma cell lines), SH-SY5Y (neuroblastoma) and SK-Br3 (breast adenocarcinoma) and non-cancerous [3 T3-L1 (pre-adipocytes); C2C12 (myo-blast); EA.hy.926 (hybrid endothelial) and SC-1 (mouse fibroblast)] cell lines, and reported that both the methanol crude extract and aqueous fractions of SADB at IC₅₀ values of 10.72 µg/mL and 17.21 µg/mL respectively, demonstrated cytotoxicity against all cell lines including DU-145 prostate carcinoma cell lines [35], which also conforms with our findings. However, the cytotoxic effects reported in their study was non-selective as it was against both cancerous and non-cancerous cell lines [35], which differs from our findings as MESADB demonstrated selective cytotoxic effects against DU-145 prostate cancer cell lines.

Also, in our study, the IC₅₀ values for the cytotoxic activities exhibited by MESADB against DU-145 cell lines was 5.11 µg/ml, which also differs from the earlier study [35]. Furthermore, three human cancer cells including lung cancer (NCI-H460), breast cancer (MCF-7), and cervical cancer (Hela) reportedly succumbed to cytotoxic effects of saponins and carpesterol from the methanol/water (80/20) extracts of SADB with IC₅₀ values ≤ 10 µg/ml in a recent study [37]. Moreso, ethanol extracts of SADB demonstrated the highest cytotoxic activity against leukemic cells with IC₅₀ of 1.36µg/ml amongst 91 Kenyan medicinal plants screened [87]. The difference in IC₅₀ values observed in these studies compared to ours may be attributed to variations in plant locations.

The phytochemical screening of the MESADB in our previous study revealed the presence of glycosides, alkaloids, steroids, terpenoids, flavonoids, phenols, tannins, and saponins [38]. These secondary metabolites could be responsible for the significant antiproliferative activities demonstrated against DU-145 prostate cancer cell lines. It is well known that flavonoids are important secondary metabolites with anticancer activities [88] amongst other medicinal properties. The anticancer activities of the terpenoids are also well documented [89]. Also, saponins have been reported to possess anticancer and apoptosis regulatory activities [90] as well as ability to lower cholesterol levels and disrupt cancer cells multiplication process [91]. Furthermore, phenols are known for their relevance in prevention and treatment of cancers and other ailments [92], and steroidal alkaloids have also been reported to possess anticancer activities [93]. Our result is supported by the outcome of previous study where two steroidal alkaloids, tomatidine and solasodine isolated from *Solanum aculeastrum* Dunal berries showed significant inhibitory activities against HT-29 (colonic adenocarcinoma), Hela (cervical adenocarcinoma) and MCF-7 (breast adenocarcinoma) cell lines by interfering with the cell cycle in the G₀/G₁ phase [32]. Although our study did not evaluate the specific mechanism of action involved in the anti-proliferative activities of MESADB against DU-145 prostate cancer cell lines, it may involve a similar mechanism of action as reported [32].

5 Conclusion

The network pharmacological screening to select drug-likeness candidate yielded three bioactive molecules which include M1, Undecane; M5, D-Arabinitol; and M11, 9-Oxabicyclo [3.3.1] nonan-2-one,6-hydroxy-. Docking outcome revealed that two [M5, D-Arabinitol; and M11, 9-Oxabicyclo [3.3.1] nonan-2-one,6-hydroxy-] out of the three bioactive compounds demonstrated strong binding affinity with two (PTGS2 and EGFR) of the hub genes. Furthermore, MESADB demonstrated significant anti-proliferative activities against DU-145 prostate cancer cells compared to negative control, which was supported by the outcome of our gene expression analysis.

Compliance with ethical standards

Acknowledgements

The authors are grateful to the Department of Biomedical Sciences and Technology, School of Public Health, and Community Development (SPHCD) and School of Graduate Studies (SGS) of Maseno University, as well as Kenya Medical Research Institute (KEMRI), Nairobi, Kenya, for their institutional support during the conduct of this study. Special appreciation to Mrs. Catherine Erosie Igben-Pender for her moral, emotional and social support during the conduct of this study.

Disclosure of conflict of interest

Authors declare no competing interests.

Statement of ethical approval

Approval was obtained from the Maseno University School of Graduate Studies (SGS), Maseno University Scientific Ethical Review Committee (MUSERC/00898/20) and the National Commission for Science, Technology, and Innovation (NACOSTI), Kenya (NACOSTI/P/21/8440).

Funding

This work did not receive external funding.

Authorship Contribution Statement

GCP, BG, PGM, and JO conceptualized the study. GCP wrote the protocol. GCP, MJ and IJLL collected the data, organized, and prepared the results. GCP wrote the first draft of the manuscript. The final manuscript was read and approved by all authors.

References

- [1] Stanković N, Mihajilov-Krstev T, Zlatković B, et al. Antibacterial and Antioxidant Activity of Traditional Medicinal Plants from the Balkan Peninsula. *NJAS - Wageningen J Life Sci* 2016; 78: 21–28.
- [2] Innocent OO, Florence AN, Mutinda CK, et al. Phytochemical screening and gas chromatography-mass spectrometry analysis of Euphorbia ingens organic root extract. *J Med Plants Res* 2023; 17: 100–105.
- [3] Wyk B Van, Wink M. *Medicinal plants of the world*, <https://books.google.com/books?hl=en&lr=&id=UAitDwAAQBAJ&oi=fnd&pg=PA3&dq=Van+Wyk+B-E,+Wink+M.+Medicinal+Plants+of+the+World.+1st+ed.+Wallingford,+UK:+CABI%3B+2018:362&ots=gqkZXXdvv&sig=3sHz-o42lwbgz0zetLiVm1Q97xk> (2018, accessed 22 January 2024).
- [4] McVary KT. BPH: Epidemiology and comorbidities. *Am J Manag Care*; 12.
- [5] Devlin C, Simms M, international NM-B, et al. Benign prostatic hyperplasia—what do we know? *Wiley Online Libr Devlin, MS Simms, NJ MaitlandBJU Int* 2021•*Wiley Online Libr* 2020; 127: 389–399.
- [6] Huang G, He X, Xue Z, et al. Rauwolfia vomitoria extract suppresses benign prostatic hyperplasia by inducing autophagic apoptosis through endoplasmic reticulum stress. *BMC Complement Med Ther*; 22. Epub ahead of print 1 December 2022. DOI: 10.1186/S12906-022-03610-4.
- [7] Song L, Shen W, Zhang H, et al. Differential expression of androgen, estrogen, and progesterone receptors in benign prostatic hyperplasia. *Bosn J basic Med Sci* 2016; 16: 201–208.
- [8] Yu ZJ, Yan HL, Xu FH, et al. Efficacy and Side Effects of Drugs Commonly Used for the Treatment of Lower Urinary Tract Symptoms Associated With Benign Prostatic Hyperplasia. *Frontiers in Pharmacology*; 11. Epub ahead of print 8 May 2020. DOI: 10.3389/fphar.2020.00658.
- [9] McVary K. Epidemiology and pathophysiology of benign prostatic hyperplasia. *Uptodate* 2021; 1–11.
- [10] Hammarsten J, pressure BH-B, 2004 undefined. Clinical, haemodynamic, anthropometric, metabolic and insulin profile of men with high-stage and high-grade clinical prostate cancer. *Taylor Fr Hammarsten, B HögstedtBlood Press* 2004•*Taylor Fr* 2009; 13: 47–55.
- [11] Ørsted DD, Bojesen SE, Nielsen SF, et al. Association of clinical benign prostate hyperplasia with prostate cancer incidence and mortality revisited: a nationwide cohort study of 3,009,258 men. *Eur Urol* 2011; 60: 691–698.
- [12] Dai X, Fang X, Ma Y, et al. Benign prostatic hyperplasia and the risk of prostate cancer and bladder cancer a meta-analysis of observational studies. *Med (United States)* 2016; 95: e3493.
- [13] Dai X, Fang X, Ma Y, et al. Benign prostatic hyperplasia and the risk of prostate cancer and bladder cancer a meta-analysis of observational studies. *Med (United States)* 2016; 95: e3493.
- [14] Sung H, Ferlay J, ... RS-C a cancer journal, et al. Global cancer statistics 2020: GLOBOCAN estimates of incidence and mortality worldwide for 36 cancers in 185 countries. *Wiley Online Libr Sung, J Ferlay, RL Siegel, M Laversanne, I Soerjomataram, A Jemal, F BrayCA a cancer J Clin* 2021•*Wiley Online Libr* 2021; 71: 209–249.
- [15] Bray F, Parkin DM, Gnanngnon F, et al. Cancer in sub-Saharan Africa in 2020: a review of current estimates of the national burden, data gaps, and future needs. *Lancet Oncol* 2022; 23: 719–728.
- [16] Ferlay J, Colombet M, Soerjomataram I, et al. Cancer statistics for the year 2020: An overview. *Int J cancer* 2021; 149: 778–789.
- [17] Alcaraz A, Hammerer P, Tubaro A, et al. Is There Evidence of a Relationship between Benign Prostatic Hyperplasia and Prostate Cancer? Findings of a Literature Review. *European Urology* 2009; 55: 864–875.

- [18] Roehrborn C. 10 The impact of acute or chronic inflammation in baseline biopsy on the risk of progression in the MTOPS study. *Eur Urol Suppl* 2005; 4: 5.
- [19] MacLennan GT, Eisenberg R, Fleshman RL, et al. The Influence of Chronic Inflammation in Prostatic Carcinogenesis: A 5-Year Followup Study. *J Urol* 2006; 176: 1012–1016.
- [20] Ozden C, Ozdal OL, Urgancioglu G, et al. The Correlation between Metabolic Syndrome and Prostatic Growth in Patients with Benign Prostatic Hyperplasia. *Eur Urol* 2007; 51: 199–206.
- [21] Madersbacher S, Sampson N, Culig Z. Pathophysiology of Benign Prostatic Hyperplasia and Benign Prostatic Enlargement: A Mini-Review. *Gerontology* 2019; 65: 458–464.
- [22] Kyprianou N, Tu H, Jacobs SC. Apoptotic versus proliferative activities in human benign prostatic hyperplasia. *Hum Pathol* 1996; 27: 668–675.
- [23] Guyatt GH, Oxman AD, Kunz R, et al. What is 'quality of evidence' and why is it important to clinicians? *BMJ* 2008; 336: 133–137.
- [24] Higgins J, medicine ST-S in, 2002 undefined. Quantifying heterogeneity in a meta-analysis. *Wiley Online Libr Higgins, SG Thompson Statistics Med 2002*•*Wiley Online Libr* 2002; 21: 1539–1558.
- [25] Soler R, Andersson KE, Chancellor MB, et al. Future direction in pharmacotherapy for non-neurogenic male lower urinary tract symptoms. *Eur Urol* 2013; 64: 610–621.
- [26] Chughtai B, Lee R, Te A, et al. Role of inflammation in benign prostatic hyperplasia. *Rev Urol* 2011; 13: 147–50.
- [27] Kapoor A. Benign prostatic hyperplasia (BPH) management in the primary care setting. *Can J Urol* 2012; 19: 10–17.
- [28] Traish AM. Negative impact of testosterone deficiency and 5 α -reductase inhibitors therapy on metabolic and sexual function in men. *Adv Exp Med Biol* 2017; 1043: 473–526.
- [29] Okaiyeto K, Oguntibeju OO. African herbal medicines: Adverse effects and cytotoxic potentials with different therapeutic applications. *Int J Environ Res Public Health*; 18. Epub ahead of print 1 June 2021. DOI: 10.3390/IJERPH18115988.
- [30] Okpako IO, Ng'ong'a FA, Kyama CM, et al. Antiproliferative activity of ethyl acetate fraction of *Euphorbia ingens* against prostate cancer cell line: An in silico and in vitro analysis. *Sci African*; 22. Epub ahead of print 2023. DOI: 10.1016/j.sciaf.2023.e01943.
- [31] Iqbal J, Abbasi BA, Mahmood T, et al. Plant-derived anticancer agents: A green anticancer approach. *Asian Pacific Journal of Tropical Biomedicine* 2017; 7: 1129–1150.
- [32] Koduru S, Grierson DS, Afolayan AJ. Ethnobotanical information of medicinal plants used for treatment of cancer in the Eastern Cape Province, South Africa. *Curr Sci* 2007; 92: 906–908.
- [33] Aboyade OM, Yakubu MT, Grierson DS, et al. Safety evaluation of aqueous extract of unripe berries of *Solanum aculeastrum* in male wistar rats. *African J Pharm Pharmacol* 2010; 4: 090–097.
- [34] Elujoba AA. Review of the Book "African Herbal Pharmacopoeia" by Brendler, T., Eloff, J. N., Gurib-Fakim, A., Phillips, L. D. Published by the Association for African Medicinal Plants Standards (2010). *African J Tradit Complement Altern Med* 2012; 9: 81.
- [35] Burger T, Mokoka T, Fouché G, et al. Solamargine, a bioactive steroidal alkaloid isolated from *Solanum aculeastrum* induces non-selective cytotoxicity and P-glycoprotein inhibition. *BMC Complement Altern Med*; 18. Epub ahead of print 2 May 2018. DOI: 10.1186/S12906-018-2208-7.
- [36] Ochwang'i DO, Kimwele CN, Oduma JA, et al. Medicinal plants used in treatment and management of cancer in Kakamega County, Kenya. *J Ethnopharmacol* 2014; 151: 1040–1055.
- [37] Tinguép Tchappnda NP, Njinkou Njambouo RB, Tchuendem Kenmogne MH, et al. Cytotoxic constituents from the fruit of *Solanum aculeastrum*. *Nat Prod Res*. Epub ahead of print 2024. DOI: 10.1080/14786419.2024.2320738.
- [38] Gift Crucifix Pender, Bernard Guyah, Peter G. Mwitari, et al. *Solanum aculeastrum* Dunal berries: Phytochemical profiling and GC-MS analysis of methanolic extract and n-hexane, dichloromethane, ethyl acetate and n-butanol fractions. *Int J Sci Res Arch* 2024; 11: 1933–1958.
- [39] Patel N, Patel SmtSSPatel LN, Patel NB, et al. ADMET & Cytotoxicity prediction of red seaweed *Gracillaria dura*: An in silico approach. *Artic World J Pharm Res* 2020; 9: 991–1004.

- [40] Soltani Rad MN, Behrouz S, Aghajani S, et al. Design, synthesis, anticancer and in silico assessment of 8-caffeinyl-triazolylmethoxy hybrid conjugates. *RSC Adv* 2023; 13: 3056–3070.
- [41] Chin CH, Chen SH, Wu HH, et al. cytoHubba: Identifying hub objects and sub-networks from complex interactome. *BMC Syst Biol*; 8. Epub ahead of print 8 December 2014. DOI: 10.1186/1752-0509-8-S4-S11.
- [42] Fischer R, Kessler BM. Gel-aided sample preparation (GASP)-A simplified method for gel-assisted proteomic sample generation from protein extracts and intact cells. *Proteomics* 2015; 15: 1224–1229.
- [43] Fu S, Zhou Y, Hu C, et al. Network pharmacology and molecular docking technology-based predictive study of the active ingredients and potential targets of rhubarb for the treatment of diabetic nephropathy. *BMC Complement Med Ther*; 22. Epub ahead of print 1 December 2022. DOI: 10.1186/S12906-022-03662-6.
- [44] Liu C, Li H, Wang K, et al. Identifying the antiproliferative effect of Astragalus polysaccharides on breast cancer: Coupling network pharmacology with targetable screening from the cancer genome atlas. *Front Oncol*; 9. Epub ahead of print 2019. DOI: 10.3389/FONC.2019.00368/FULL.
- [45] Wang D, Zhang Y, Wang X, et al. Construction and validation of an aging-related gene signature predicting the prognosis of pancreatic cancer. *Front Genet*; 14. Epub ahead of print 18 January 2023. DOI: 10.3389/fgene.2023.1022265.
- [46] Khatibi S, Farzaneh Taban Z, Mohammadi Roushandeh A. In Vitro Evaluation of Cytotoxic and Antiproliferative Effects of Portulaca oleracea Ethanolic Extracton on HeLa Cell Line. *Gene, Cell Tissue*; 4. Epub ahead of print 2016. DOI: 10.17795/gct.41565.
- [47] Eghianruwa Q, Osoniyi O, Wachira S, et al. In vitro antiproliferative studies of extracts of the marine molluscs: Tympanotonus fuscatus Var radula (linnaeus) and Pachymelania aurita (muller). *Int J Biochem Mol Biol* 2019; 10: 1–8.
- [48] Sergazy S, Vetrova A, Orhan IE, et al. Antiproliferative and cytotoxic activity of Geraniaceae plant extracts against five tumor cell lines. *Futur Sci Sergazy, A Vetrova, IE Orhan, FS Senol Deniz, A Kahraman, JY Zhang, M AljofanFuture Sci OA, 2022•Future Sci*; 8. Epub ahead of print 1 February 2021. DOI: 10.2144/fsoa-2021-0109.
- [49] Kimani PM, Mwitari PG, Mwenda Njagi S, et al. In Vitro Anti-Proliferative Activity of Selected Plant Extracts Against Cervical and Prostate Cancer Cell Lines. *J Cancer Sci Ther*; 10. Epub ahead of print 2018. DOI: 10.4172/1948-5956.1000555.
- [50] Lubrano C, Toscano V, Petrangeli E, et al. Relationship between epidermal growth factor and its receptor in human benign prostatic hyperplasia. *J Steroid Biochem Mol Biol* 1993; 46: 463–468.
- [51] Olapade-Olaopa EO, Moscatello DK, MacKay EH, et al. Evidence for the differential expression of a variant EGF receptor protein in human prostate cancer. *Br J Cancer* 2000; 82: 186–194.
- [52] khudhair muneer kadhem. Validation Gene Expression of Rna-Binding Proteins and Biomarkers in Benign Prostatic Hyperplasia and Prostate Cancer, https://www.academia.edu/64879654/Validation_Gene_Expression_of_Rna_Binding_Proteins_and_Biomarkers_in_Benign_Prostatic_Hyperplasia_and_Prostate_Cancer (2021, accessed 20 March 2024).
- [53] Ke Z Bin, Cai H, Wu YP, et al. Identification of key genes and pathways in benign prostatic hyperplasia. *J Cell Physiol* 2019; 234: 19942–19950.
- [54] Chen KC, Peng CC, Peng CH, et al. The aqueous soluble polyphenolic fraction of Psidium guajava leaves exhibits potent anti-angiogenesis and anti-migration actions on DU145 cells. *Evidence-based Complement Altern Med*; 2011. Epub ahead of print 2011. DOI: 10.1093/ecam/neq005.
- [55] Hla T, Bishop-Bailey D, Liu CH, et al. Cyclooxygenase-1 and -2 isoenzymes. *Int J Biochem Cell Biol* 1999; 31: 551–557.
- [56] Liu XH, Yao S, Kirschenbaum A, et al. NS398, a selective cyclooxygenase-2 inhibitor, induces apoptosis and down-regulates bcl-2 expression in LNCaP cells. *Cancer Res* 1998; 58: 4245–4249.
- [57] Wang MT, Honn K V., Nie D. Cyclooxygenases, prostanoids, and tumor progression. *Cancer Metastasis Rev* 2007; 26: 525–534.
- [58] Gupta S, Srivastava M, Ahmad N, et al. Over-expression of cyclooxygenase-2 in human prostate adenocarcinoma. *Prostate* 2000; 42: 73–78.

- [59] Uotila P, Valve E, Martikainen P, et al. Increased expression of cyclooxygenase-2 and nitric oxide synthase-2 in human prostate cancer. *Urol Res* 2001; 29: 25–28.
- [60] Kim BH, Kim C Il, Chang HS, et al. Cyclooxygenase-2 overexpression in chronic inflammation associated with benign prostatic hyperplasia: Is it related to apoptosis and angiogenesis of prostate cancer? *Korean J Urol* 2011; 52: 253–259.
- [61] Fernández-Martínez AB, Carmena MJ, Isabel Arenas M, et al. Overexpression of vasoactive intestinal peptide receptors and cyclooxygenase-2 in human prostate cancer. Analysis of potential prognostic relevance. *Histol Histopathol* 2012; 27: 1093–1101.
- [62] Lou W, Ni Z, Dyer K, et al. Interleukin-6 Induces Prostate Cancer Cell Growth Accompanied by Activation of Stat3 Signaling Pathway. *Prostate* 2000; 42: 239–242.
- [63] Frannata L, Soerohardjo I, Danarto R, et al. Overexpression of Estrogen Receptor 1 (ESR-1) in metastatic prostate cancer. *ijbs-udayana.org L Frannata, EK Dwianingsih, R Danarto Indonesia J Biomed Sci 2022 • ijbs-udayana.org* 2022; 16: 47–50.
- [64] Richter CA, Taylor JA, Ruhlen RL, et al. Estradiol and bisphenol A stimulate androgen receptor and estrogen receptor gene expression in fetal mouse prostate mesenchyme cells. *Environ Health Perspect* 2007; 115: 902–908.
- [65] Sun Y, Ai JZ, Jin X, et al. IL-8 protects prostate cancer cells from GSK-3 β -induced oxidative stress by activating the mTOR signaling pathway. *Prostate* 2019; 79: 1180–1190.
- [66] Heinlein CA, Chang C. Androgen receptor (AR) coregulators: An overview. *Endocrine Reviews* 2002; 23: 175–200.
- [67] McKenna NJ, Lanz RB, O'Malley BW. Nuclear receptor coregulators: Cellular and molecular biology. *Endocrine Reviews* 1999; 20: 321–344.
- [68] Powell SM, Christiaens V, Voulgaraki D, et al. Mechanisms of androgen receptor signalling via steroid receptor coactivator-1 in prostate. *Endocrine-Related Cancer* 2004; 11: 117–130.
- [69] Gregory CW, He B, Johnson RT, et al. A mechanism for androgen receptor-mediated prostate cancer recurrence after androgen deprivation therapy. *Cancer Res* 2001; 61: 4315–4319.
- [70] Yang J, Wang L, Wu MX. 830 nm photobiomodulation therapy promotes engraftment of human umbilical cord blood-derived hematopoietic stem cells. *Sci Rep*; 10. Epub ahead of print 2020. DOI: 10.1038/s41598-020-76760-5.
- [71] Saraav I, Singh S, biology SS-I and cell, et al. Outcome of Mycobacterium tuberculosis and Toll-like receptor interaction: immune response or immune evasion? *Wiley Online Libr Saraav, S Singh, S Sharma Immunology cell Biol 2014 • Wiley Online Libr* 2014; 92: 741–746.
- [72] O'Neill LAJ, Golenbock D, Bowie AG. The history of Toll-like receptors-redefining innate immunity. *Nature Reviews Immunology* 2013; 13: 453–460.
- [73] Mäkinen LK, Atula T, Häyry V, et al. Predictive role of toll-like receptors 2, 4, and 9 in oral tongue squamous cell carcinoma. *Oral Oncol* 2015; 51: 96–102.
- [74] Parker LC, Prince LR, Sabroe I. Translational mini-review series on Toll-like receptors: Networks regulated by Toll-like receptors mediate innate and adaptive immunity. *Clin Exp Immunol* 2007; 147: 199–207.
- [75] Liu H, Komai-Koma M, Xu D, et al. Toll-like receptor 2 signaling modulates the functions of CD4 +CD25+ regulatory T cells. *Proc Natl Acad Sci U S A* 2006; 103: 7048–7053.
- [76] den Dekker WK, Cheng C, Pasterkamp G, et al. Toll like receptor 4 in atherosclerosis and plaque destabilization. *Atherosclerosis* 2010; 209: 314–320.
- [77] Qiu Y, Zheng J, Yang J, et al. The predictive role of toll-like receptor-4 genetic polymorphisms in susceptibility to and prognosis of prostatic hyperplasia. *Iran J Basic Med Sci* 2019; 22: 86–92.
- [78] Wang D, Liu K, Wake H, et al. Anti-high mobility group box-1 (HMGB1) antibody inhibits hemorrhage-induced brain injury and improved neurological deficits in rats. *Sci Rep*; 7. Epub ahead of print 2017. DOI: 10.1038/srep46243.
- [79] Jain S, Dash P, Minz AP, et al. Lipopolysaccharide (LPS) enhances prostate cancer metastasis potentially through NF- κ B activation and recurrent dexamethasone administration fails to suppress it in vivo. *Prostate* 2019; 79: 168–182.

- [80] Oseni SO, Naar C, Pavlović M, et al. The Molecular Basis and Clinical Consequences of Chronic Inflammation in Prostatic Diseases: Prostatitis, Benign Prostatic Hyperplasia, and Prostate Cancer. *Cancers*; 15. Epub ahead of print 2023. DOI: 10.3390/cancers15123110.
- [81] Dobosy JR, Roberts JLW, Fu VX, et al. The Expanding Role of Epigenetics in the Development, Diagnosis and Treatment of Prostate Cancer and Benign Prostatic Hyperplasia. *J Urol* 2007; 177: 822–831.
- [82] Patra SK, Patra A, Dahiya R. Histone deacetylase and DNA methyltransferase in human prostate cancer. *Biochem Biophys Res Commun* 2001; 287: 705–713.
- [83] Halkidou K, Gaughan L, Cook S, et al. Upregulation and nuclear recruitment of HDAC1 in hormone refractory prostate cancer. *Wiley Online Libr Halkidou, L Gaughan, S Cook, HY Leung, Neal, CN RobsonThe Prostate, 2004•Wiley Online Libr* 2004; 59: 177–189.
- [84] Li Y, Zhang C, Ma X, et al. Identification of the potential mechanism of Radix pueraria in colon cancer based on network pharmacology. *Sci Rep*; 12. Epub ahead of print 2022. DOI: 10.1038/s41598-022-07815-y.
- [85] Sharma R, Jadhav M, Choudhary N, et al. Deciphering the impact and mechanism of Trikatu, a spices-based formulation on alcoholic liver disease employing network pharmacology analysis and in vivo validation. *Front Nutr*; 9. Epub ahead of print 16 November 2022. DOI: 10.3389/fnut.2022.1063118.
- [86] Canga I, Vita P, Oliveira AI, et al. In Vitro Cytotoxic Activity of African Plants: A Review. *Molecules*; 27. Epub ahead of print 1 August 2022. DOI: 10.3390/MOLECULES27154989.
- [87] Omosa LK, Midiwo JO, Masila VM, et al. Cytotoxicity of 91 Kenyan indigenous medicinal plants towards human CCRF-CEM leukemia cells. *J Ethnopharmacol* 2016; 179: 177–196.
- [88] Bassiouni W, Daabees T, Louedec L, et al. Evaluation of some prostaglandins modulators on rat corpus cavernosum in-vitro: Is relaxation negatively affected by COX-inhibitors? *Biomed Pharmacother* 2019; 111: 1458–1466.
- [89] Ramawat KG, Mérillon JM. Natural Products: Phytochemistry, Botany and Metabolism of Alkaloids, Phenolics and Terpenes. *Nat Prod* 2013; 1–4242.
- [90] Zhong J, Tan L, Chen M, et al. Pharmacological activities and molecular mechanisms of Pulsatilla saponins. *Chinese Med (United Kingdom)*; 17. Epub ahead of print 1 December 2022. DOI: 10.1186/S13020-022-00613-8.
- [91] Jesch ED, Carr TP. Food ingredients that inhibit cholesterol absorption. *Preventive Nutrition and Food Science* 2017; 22: 67–80.
- [92] Pinto T, Aires A, Cosme F, et al. Bioactive (poly) phenols, volatile compounds from vegetables, medicinal and aromatic plants. *mdpi.comT Pinto, A Aires, F Cosme, E Bacelar, MC Morais, I Oliveira, J Ferreira-Cardoso, R AnjosFoods, 2021•mdpi.com*. Epub ahead of print 2021. DOI: 10.3390/foods10010106.
- [93] M M, J R, V L, et al. Natural and Synthetic Derivatives of the Steroidal Glycoalkaloids of Solanum Genus and Biological Activity. *Nat Prod Chem Res* 2020; 8: 1–14.